Polymer Chain Length Dependence of Amplified Fluorescence Quenching in Conjugated Polyelectrolytes

Xiaoyong Zhao, Hui Jiang, and Kirk S. Schanze*

Department of Chemistry, University of Florida, P.O. Box 117200, Gainesville, Florida 32611-7200

Received January 26, 2008; Revised Manuscript Received March 4, 2008

ABSTRACT: This paper reports the synthesis and photophysical study of a series of anionic, carboxylate-substituted poly(phenylene ethynylene)-based conjugated polyelectrolytes (CPEs) with variable chain lengths. These CPEs are of interest as they allow the study of the effect of chain length on amplified fluorescence quenching. The CPEs were synthesized via organic soluble ester precursor polymers. The degree of polymerization of the precursor polymers was controlled by addition of a monofunctional "end-cap" to the polymerization reaction. The CPEs were obtained postpolymerization by base-promoted hydrolysis of the ester protecting groups. Stern−Volmer fluorescence quenching of the CPEs in methanol with monovalent electron-transfer quenchers (MV^+ and HV^+) show that the Stern−Volmer quenching constant (K_{SV}) increases with polymer chain length reaching a maximum of ca. 2×10^5 M^{-1} at a degree of polymerization of 49. The results indicate that a maximum quenching amplification factor of 53 is attained under conditions where monovalent quencher ions interact with nonaggregated (single) polymer chains.

Introduction

Since the first report of sulfonate-substituted polythiophenes,[1] water-soluble conjugated polyelectrolytes (CPEs) have been studied for almost two decades. One of the most important developments in the area was the discovery of a million-fold amplification of the fluorescence quenching sensitivity of poly(2-methoxy-5-propyloxysulfonate phenylenevinylene) (MPS−PPV) by methyl viologen (MV^{2+}) compared with quenching of stilbene.[2] This finding stimulated substantial investigation of photophysical properties of CPEs by interaction with various aqueous soluble species, such as metal ions,[3,4] organic ions,[2,5–8] dendrimers,[9] small biomolecules,[2] proteins,[10] and nanoparticles.[11] The ability of such ionic species to quench the fluorescence of oppositely charged CPEs with extraordinary efficiency has been termed "amplified quenching"[12] or "superquenching".[2]

The efficiency of fluorescence quenching is quantitatively evaluated by the Stern−Volmer (SV) equation[13]

$$I_0/I = 1 + K_{SV}[Q]$$

where I and I_0 are the fluorescence intensity with and without the quencher, respectively, [Q] is quencher concentration, and K_{SV} is the Stern−Volmer constant. For diffusion-controlled quenching of small uncharged fluorophores K_{SV} ranges from 10^0 to 10^1 M^{-1}, and the values increase to 10^2-10^3 M^{-1} when the fluorophore and quencher are oppositely charged ions. By contrast, Stern−Volmer constants on the order of 10^6-10^9 M^{-1} are reported for quenching of CPEs by oppositely charged ions. The mechanism of the highly efficient quenching of CPEs has been attributed to a combination of several different features, i.e., ion-pair complex formation between the polymer and the quencher,[2,7,11,14] efficient intrachain exciton diffusion along the polymer chain,[2,7,15,16] 3-dimensional interchain exciton diffusion in CPE aggregates,[2,14,17] and ultrafast charge/energy transfer between the polymer and the quencher.[2,17]

In studies directed toward elucidating the mechanism of amplified quenching, the photophysical properties and quenching efficiencies of CPEs have been shown to be strongly influenced by polymer concentration,[16] quencher properties (charge,[7] hydrophobicity,[8] size[18]), solution properties (pH,[5,19] ionic strength,[6,19] buffer[6]), and interaction with surfactants[16,20,21] and other species.[22,23] However, while the optical properties of many series of conjugated oligomers as a function of chain length have been studied,[24] the relationship(s) between photophysical properties, quenching behavior, and CPE molecular weight (chain length) have not been studied systematically. In an early report of a series of receptor-substituted organic soluble (neutral) polymers Zhou and Swager showed that K_{SV} increases with polymer chain length in low molecular weight samples (M_n < 65 kDa); however, for samples with higher molecular weight K_{SV} only increases marginally.[25] Although several other studies have shown that chain length has an effect on CPE quenching efficiency, the conclusions were based on comparison of the quenching efficiency of a limited number of samples.[15,26] Thus, a systematic study using a series of CPEs in which the molecular weight is varied systematically is required to obtain clear insight as to how fluorescence quenching efficiency varies with CPE chain length.

Herein, we report the chain length dependence of the fluorescence quenching efficiency of a series of carboxylate-substituted (anionic) poly(*p*-phenylene ethynylene)s by monovalent cationic quenchers. The series of anionic CPEs were synthesized via a "precursor route" in which the carboxyl groups were protected as long chain esters, making the polymers soluble in organic solvents. The molecular weight of the organic soluble polymer precursors was systematically controlled by addition of precise amounts of a monofunctional "end-capping" agent to the polymerization reaction mixture. After polymerization, the molecular weight distribution of each ester protected polymer sample was determined by gel permeation chromatography (GPC) and NMR end-group analysis. Subsequent to the analysis, the corresponding series of water-soluble CPEs were obtained by base-catalyzed hydrolysis of the ester precursors. The series of CPEs were then subjected to a systematic photophysical investigation in methanol and water solutions, including the study of the dependence of the fluorescence quenching efficiency on CPE chain length. The results of this study provide considerable insight concerning the relationship between CPE chain length and the amplified quenching effect.

Experimental Section

Instrumentation. NMR spectra were obtained with a Varian Mecury-300 or a Varian Gemini-300, and chemical shifts are

* Corresponding author: Tel 352-392-9133; e-mail kschanze@chem.ufl.edu.

10.1021/ma800191q CCC: $40.75
Published on Web 04/25/2008

reported in ppm using $CHCl_3$ or CD_3SOCHD_2 as the internal reference. In the ^{19}F NMR experiments, octafluoro[2.2]paracyclophane was used as the internal reference.[27] Gel permeation chromatography (GPC) analyses were carried out on a system comprised of a Rainin Dynamax SD-200 pump, Polymer Laboratories PLgel mixed D columns, and a Beckman Instruments Spectroflow 757 absorbance detector. Molecular weight calibration was effected by using polystyrene standards. UV−vis absorption spectra were recorded using a Lambda 25 spectrophotometer from Perkin-Elmer. Steady-state fluorescence spectra were obtained with a Fluorolog 3 spectrofluorimeter from JY SPEX. A 1 cm square quartz cuvette was used for all spectral measurements. Fluorescence quantum yields were measured relative to a coumarin 102 standard (λ_{exc} = 380 nm and $\Phi_{em} = 0.67$ in EtOH).[28]

Materials. Triethylamine and tetrahydrofuran (THF) were purified by distillation over sodium hydride. $Pd(PPh_3)_4$ catalyst was used as received from Strem Chemical Co. 2,5-Bis(dodecyloxycarbonylmethoxy)-1,4-diiodobenze (**1**) and 1,4-diethynylbenzene (**2**) were synthesized by revised procedures reported in the literature[29] (see Supporting Information for details). 1-Iodo-4-(trifluoromethyl)benzene, *N,N*-dimethyl-4,4′-bipyridinium chloride (MV^{2+}), and *N,N*-heptyl-4,4′-bipyridinium bromide (HV^{2+}) were purchased from Sigma-Aldrich and used without further purification. *N*-Heptyl-4,4′-bipyridinium bromide (HV^{+}) was purchased from Sigma-Aldrich and further purified by recrystallization from acetone.[30] *N*-Methyl-4,4′-bipyridinium iodide (MV^{+}) was synthesized following a literature procedure.[31]

Synthetic Procedures. Polymerization. Monomer **1** (407.3 mg, 0.50 mmol), monomer **2** (63.1 mg, 0.50 mmol), and a specific amount of 1-iodo-4-(trifluoromethyl)benzene (**3**, varying from 1% to 25%, molar ratio) were dissolved in 20 mL of a dry THF/Et_3N (3/2) mixture in a Schlenk flask. The solution was deoxygenated with argon for 15 min at 55 °C. Then $Pd(PPh_3)_4$ (16.2 mg, 0.014 mmol) and CuI (5.0 mg, 0.026 mmol) were added into the solution under the protection of argon. The resulting mixture was heated to 60 °C and stirred for 24 h. The obtained yellow solution was poured into methanol (200 mL), which induced the polymer to precipitate. The precipitate was collected by vacuum filtration and further purified by two repeated cycles of dissolution in THF and precipitation into a large volume of methanol. A typical reaction yield was 80%−85%.

PPE-CO_2R-7. GPC (THF, polystyrene standard): M_w = 9500, M_n = 5390, PDI = 1.80. ^1H NMR ($CDCl_3$, δ_{ppm}): 7.64 (end groups), 7.56 (br, m, 4H), 7.02 (s, 2H), 4.74 (s, 4H), 4.24 (t, 4H), 1.68 (m, 4H), 1.31−1.25 (m, 36H), 0.90 (t, 6H). ^{19}F NMR ($CDCl_3$, δ_{ppm}): −63.22, −118.63 (internal standard). FT-IR (ν_{max}, KBr pellet): 3041, 2925, 2854, 2208, 1762, 1733, 1614, 1520, 1489, 1468, 1439, 1412, 1323, 1282, 1188, 1081,839, 722, 598, 544.

PPE-CO_2R-13. GPC (THF, polystyrene standard): M_w = 20 640, M_n = 9040, PDI = 2.30. ^1H NMR ($CDCl_3$, δ_{ppm}): 7.64 (end groups), 7.56 (br, m, 4H), 7.02 (s, 2H), 4.74 (s, 4H), 4.24 (t, 4H), 1.68 (m, 4H), 1.31−1.26 (m, 36H), 0.90 (t, 6H). ^{19}F NMR ($CDCl_3$, δ_{ppm}): −63.22, −118.63 (internal standard). FT-IR (ν_{max}, KBr pellet): 3040, 2925, 2854, 2207, 1761, 1738, 1615, 1520, 1490, 1467, 1440, 1412, 1377, 1323, 1282, 1188, 1130, 1082, 1017, 837, 722, 544.

PPE-CO_2R-35. GPC (THF, polystyrene standard): M_w = 56 980, M_n = 24 390, PDI = 2.30. ^1H NMR ($CDCl_3$, δ_{ppm}): 7.64 (end groups), 7.56 (br, m, 4H), 7.02 (s, 2H), 4.74 (s, 4H), 4.24 (t, 4H), 1.68 (m, 4H), 1.31−1.26 (m, 36H), 0.90 (t, 6H). ^{19}F NMR ($CDCl_3$, δ_{ppm}): −63.22, −118.63 (internal standard).

PPE-CO_2R-49. GPC (THF, polystyrene standard): M_w = 78 750, M_n = 33 760, PDI = 2.30. ^1H NMR ($CDCl_3$, δ_{ppm}): 7.56 (br, m, 4H), 7.02 (s, 2H), 4.74 (s, 4H), 4.24 (t, 4H), 1.68 (m, 4H), 1.31−1.26 (m, 36H), 0.90 (t, 6H). ^{19}F NMR ($CDCl_3$, δ_{ppm}): −63.22, −118.63 (internal standard).

PPE-CO_2R-108. GPC (THF, polystyrene standard): M_w = 202 890, M_n = 74 350, PDI = 2.70. ^1H NMR ($CDCl_3$, δ_{ppm}): 7.55 (br, m, 4H), 7.02 (s, 2H), 4.74 (s, 4H), 4.24 (t, 4H), 1.68 (m, 4H), 1.31−1.26 (m, 36H), 0.90 (t, 6H). ^{19}F NMR ($CDCl_3$, δ_{ppm}): −63.22, −118.63 (internal standard).

Hydrolysis. A small amount (∼30 mg) of sample was taken from the obtained organic soluble ester polymers and used for GPC and NMR characterization. The remaining material was dissolved in ∼40 mL of 1,4-dioxane. To the solution, 4 mL of (n-Bu)$_4$NOH solution (1 M in methanol) was added. The solution became turbid immediately upon the addition of the base. Water (4 mL) was added at this stage whereupon the mixture became clear and was stirred at room temperature for 24 h. Then a solution of sodium perchlorate (480 mg, 4 mmol) dissolved in 1 mL of water was added to the hydrolyzed polymer solution, and the resulting mixture was poured into 500 mL of cold acetone, at which point the water-soluble polymer precipitated as a fine yellow powder. Final purification of the polymers was accomplished by dialysis of the aqueous solution of the polymer against pure water (Millipore Simplicity water system), and using a 12 kDa molecular weight cutoff (MWCO) regenerated cellulose membrane (Fisher Scientific). After dialysis, the solution was filtered through a 1.0 μm glass fiber membrane, and the concentration of the aqueous solution was calibrated using gravimetric analysis. The polymers were stored in this format and diluted as appropriate for spectroscopic studies. Typical reaction yield is 90%−95%.

PPE-CO_2Na-7. ^1H NMR (D_2O/DMSO-d_6 = 1/1, δ_{ppm}): 7.66 (end groups), 7.54 (s, 4H), 7.02 (s, 2H), 4.35 (s, 4H). FT-IR (ν_{max}, KBr pellet): 3383, 2204, 1599, 1404, 1324, 1282, 1208, 1125, 1104, 1051, 943, 840, 765, 677, 597, 547.

PPE-CO_2Na-13. ^1H NMR (D_2O/DMSO-d_6 = 1/1, δ_{ppm}): 7.68 (end groups), 7.55 (s, 4H), 6.96 (s, 2H), 4.34 (s, 4H). FT-IR (ν_{max}, KBr pellet): 3401, 2927, 2255, 2205, 2127, 1607, 1515, 1488, 1404, 1323, 1281, 1205, 1126, 1104, 1049, 1025, 882, 838, 763, 703, 591, 541.

PPE-CO_2Na-35. ^1H NMR (D_2O/DMSO-d_6 = 1/1, δ_{ppm}): 7.66 (end groups), 7.54 (s, 4H), 6.98 (s, 2H), 4.39 (s, 4H). FT-IR (ν_{max}, KBr pellet): 3394, 2929, 2256, 2205, 2128, 1607, 1515, 1489, 1404, 1323, 1281, 1206, 1105, 1051, 1026, 1006, 882, 840, 825, 763, 721, 703, 614, 596, 546.

PPE-CO_2Na-49. ^1H NMR (D_2O/DMSO-d_6 = 1/1, δ_{ppm}): 7.54 (s, 4H), 6.97 (s, 2H), 4.37 (s, 4H). FT-IR (ν_{max}, KBr pellet): 3384, 2934, 2255, 2204, 2127, 1604, 1515, 1488, 1404, 1323, 1281, 1207, 1104, 1050, 1026, 1005, 884, 840, 825, 763, 720, 704, 629, 595, 545.

PPE-CO_2Na-108. ^1H NMR (D_2O/DMSO-d_6 = 1/1, δ_{ppm}): 7.55 (s, 4H), 6.96 (s, 2H), 4.34 (s, 4H). FT-IR (ν_{max}, KBr pellet): 3398, 2930, 2256, 2205, 2128 1602, 1515, 1489, 1406, 1323, 1281, 1198, 1094, 1051, 1026, 1004, 885, 841, 825, 764, 721, 700, 631, 617, 544.

Results and Discussion

Synthesis and Characterization of Ester Precursor Polymers. The structures of the monomers and polymers used in the work are shown in Scheme 1. The difunctional comonomers 2,5-bis(dodecyloxycarbonylmethoxy)-1,4-diiodobenze (**1**) and 1,4-diethynylbenzene (**2**) were polymerized in the presence of 1-iodo-4-(trifluoromethyl)benzene (**3**) as a monofunctional end-capping agent. The amount of the end-capping agent in the reaction mixture controls and limits the polymerization of the difunctional monomers, affording the ability to synthesize a homologous series of polymers with controlled and variable molecular weight. In order to minimize the influence of other factors on the chain length, all of the polymerization reactions were carried out under identical conditions in a mixture of THF/Et_3N (v/v, 3/2) with the difunctional monomer concentrations maintained at 25 mM.

Since the Pd-catalyzed (Sonogashira) polycondensation reaction proceeds via a step-growth mechanism, the degree of polymerization (DP) varies inversely with the extent of the reaction (p) by the expression DP = 1/(1 − p) (assuming that two reactive functional groups are present in a stoichiometric balance).[32] In order to compute the parameter p, we initially carried out a polymerization using **1** and **2** (1:1, molar ratio)

Scheme 1

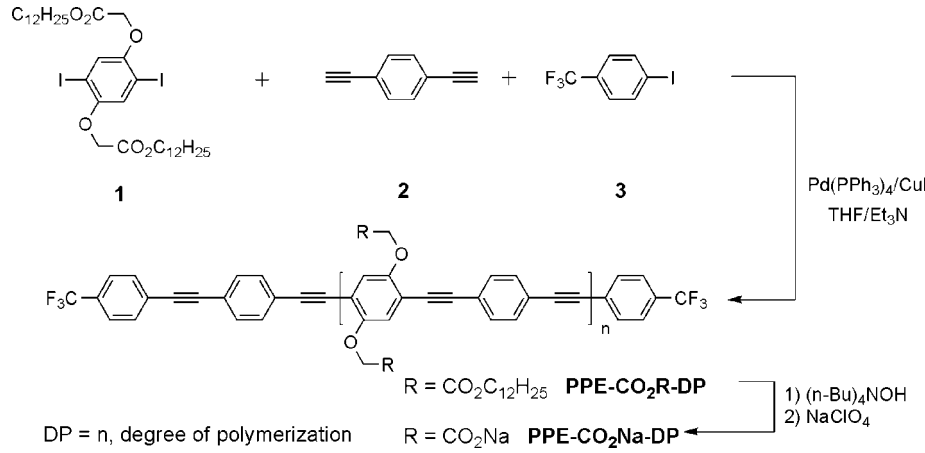

Table 1. GPC and ^{1}H NMR End-Group Analysis of Precursor Polymers

			GPC			
	end-cap (%)[a]	[DP][b]	M_n	DP	PDI	NMRDP
PPE-CO_2R-7	25	9	5 390	7	1.80	7
PPE-CO_2R-13	15	14	9 040	13	2.30	12
PPE-CO_2R-35	5	33	24 390	35	2.30	21
PPE-CO_2R-49	3	51	33 750	49	2.30	28
PPE-CO_2R-108	1	100	74 350	108	2.70	85
PPE-CO_2R-187	0		127 950	187	2.90	

[a] Molar percent. [b] DP calculated using Carothers' equation: $DP = (1 + r)/(1 + r - 2rp)$, where r = stoichiometric imbalance and p = extent of reaction.

without addition of the end-capping agent (**3**). The polymerization was monitored by using GPC, and the temporal variation of the chromatograms was consistent with a step-growth polymerization mechanism. The number-average molecular weight of the final polymer produced in this reaction was 127 900, corresponding to a DP of 187 (GPC using polystyrene standards). By using this DP value, the extent of polymerization (p) was estimated to be 0.995 by using a rearranged form of the previous expression, $p = 1 - 1/DP$. Now, by assuming this p value will hold for all the polymerizations, Carothers' equation[32] was used to predict the DP values for the polymers produced in the presence of varying amounts of the end-capping agent **3**, and the values are listed in Table 1 (column 3).

The end-capped polymers were produced by reaction of **1** and **2** in the presence of **3** (1−25 mol %), and the molecular weights of the resulting materials were determined by GPC. Representative GPC traces for all of the end-capped polymers are illustrated in Figure 1; the chromatograms clearly demonstrate that the polymers exhibit monomodal molecular weight distributions and that the degree of polymerization increases with decreasing mol % of **3** added. The number-average molecular weights (M_n) and DP values for the polymer samples determined by GPC are listed in Table 1 (columns 4 and 5). Note that there is excellent correspondence between the measured and predicted DP values, suggesting that the polymers are functionalized at both ends with end-cap **3**. The polydispersity indices (PDI) of all the polymers are ∼2, consistent with a Flory−Schulz distribution of the molecular weight for ideal step-growth polycondensation.[33] Throughout the remainder of the text, the organic soluble (ester protected) polymers are referred to using the acronym PPE-CO_2R-DP (R for organic precursors, where DP is the degree of polymerization of the sample).

Each of the PPE-CO_2R samples was also characterized by ^{1}H NMR spectroscopy in order to confirm structure and purity as well as allowing independent confirmation of the DP values. As an example, the complete ^{1}H NMR spectrum of PPE-CO_2R-7 is shown in Figure 2a (the spectra of all of the other polymer samples are provided in the Supporting Information, Figures S1−S4). The singlet at 4.73 ppm (d) is assigned to the methylene group protons (−O$CH_2CO_2C_{12}H_{25}$−), and the other signals in the aliphatic region (e, f, g, h) are due to the dodecyl chains. The aromatic protons on the 4-trifluoromethylphenyl end groups appear as a singlet at 7.64 ppm (a), and the aromatic protons on the 1,4-phenylene and 2,5-disubstituted-1,4-phenylene moieties appear at 7.56 ppm (b) and 7.02 ppm (c), respectively.

A number of studies have shown that GPC analysis (polystyrene standards) of rigid-rod polymers such as the PPE-CO_2R series overestimates M_n by a factor of 1.4−2.0.[34–36] Thus, in order to provide more information concerning the molecular weights of the PPE-CO_2R-DP series, NMR end-group analysis was used to independently evaluate the M_n values. Figure 2b shows the expanded aromatic region of the ^{1}H NMR spectra of the PPE-CO_2R series. Note that as the molecular weight increases, the signal at 7.56 ppm (b) corresponding to the 1,4-phenylene repeat units becomes broader and begins to overlap the signal for the 4-trifluoromethylphenyl end groups (a, 7.64 ppm). By contrast, the signal from the 2,5-disubstituted-1,4-phenylene repeat units (c, 7.02 ppm) is well separated from the end-group signal at 7.64 ppm. Accordingly, the DPs values for the polymers were computed by comparing the integration at 7.64 ppm (a) to the integration at 7.02 ppm (c), and the results are listed in Table 1 (column 7). Interestingly, the DP values calculated by ^{1}H NMR vs GPC differ by a factor of ∼1.5 for medium to high molecular weight samples (DP = 35, 49, 108)

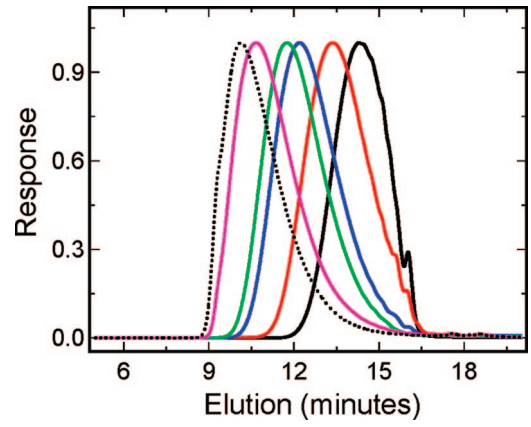

Figure 1. GPC traces of the precursor polymers. Solid lines: black, PPE-CO_2R-7; red, PPE-CO_2R-13; blue, PPE-CO_2R-35; green, PPE-CO_2R-49; purple, PPE-CO_2R-108. Black dotted line: PPE-CO_2R-187.

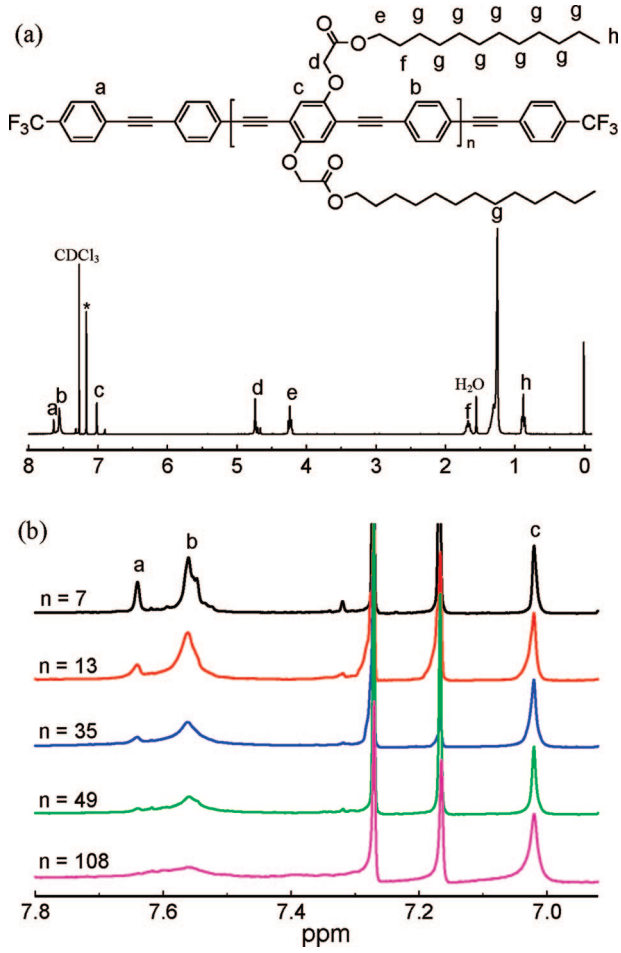

Figure 2. (a) ^{1}H NMR spectrum of PPE-CO_2R-7 in $CDCl_3$. The (*) labeled signal at 7.17 ppm is from the internal standard added for ^{19}F NMR study. (b) Expanded aromatic region ^{1}H NMR spectra of the PPE-CO_2R series in $CDCl_3$ solution.

and are approximately the same for the low molecular weight polymers (DP = 7, 13). These findings are consistent with observations made by other groups.[37–40]

The water-soluble CPEs were prepared by base-promoted hydrolysis of the PPE-CO_2R series according to a procedure previously reported by our group (Scheme 1).[29] (The resulting polymers are referred to with the acronym PPE-CO_2Na-DP, where DP is the DP value of the corresponding PPE-CO_2R-DP that was subjected to hydrolysis.) After hydrolysis, the PPE-CO_2Na series was characterized by ^{1}H NMR and IR spectroscopy (Figure S5). The ^{1}H NMR spectra of all the polymers in the D_2O/DMSO-d_6 mixture (v/v, 1/1) feature only one signal in the aliphatic region at $\delta = 4.35$ ppm corresponding to the methylene groups ($-OCH_2CO_2Na-$). This finding confirms that the ester groups are effectively removed by the hydrolysis procedure (e.g., >95% conversion).

Photophysics of Conjugated Polyelectrolytes. The absorption and fluorescence spectra of the highest molecular weight CPE (PPE-CO_2Na-187) in MeOH and H_2O were reported previously.[41] Figure 3a illustrates the absorption and emission spectra of the other five CPEs in MeOH solution. Across the series, the absorption maximum for the long-axis polarized $\pi \rightarrow \pi^*$ transition red-shifts with increasing chain length from 404 nm (PPE-CO_2Na-7), to 411 nm (PPE-CO_2Na-13), to 417 nm (PPE-CO_2Na-35). This shift is likely due to the fact that the average conjugation length increases with polymer chain length. The effect of chain length on the absorption maximum has been well documented in studies of monodisperse oligomers.[24,42] For the PPE-CO_2Na series, the extension of conjugation saturates at this point. Additional increase of the polymer molecular weight leads to the appearance of a red-shifted shoulder (432 nm, PPE-CO_2Na-49) which becomes the absorption maximum in PPE-CO_2Na-108. On the basis of our earlier studies of poly(phenylene ethynylene)s with sulfonate[14] or carboxylate side groups,[41] along with the work of others,[43] the red-shifted band at 432 nm is assigned to planarization of phenylene ethynylene backbone driven by aggregation. It is also interesting to note that there is a general trend across the series that the molar absorption coefficient (per polymer repeat unit) increases with molecular weight (Table 2). (This trend is not followed for PPE-CO_2Na-49 and PPE-CO_2Na-108 possibly because of the onset of aggregation which causes the absorption bandwidth to increase with the onset of the red-shifted shoulder absorption.)

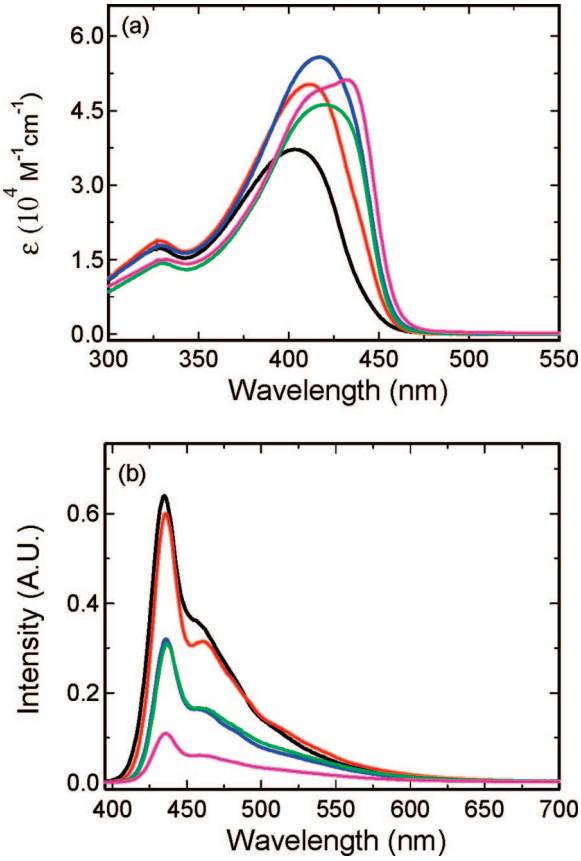

Figure 3. (a) Absorption and (b) emission spectra for methanol solutions: black, PPE-CO_2Na-7; red, PPE-CO_2Na-13; blue, PPE-CO_2Na-35; green, PPE-CO_2Na-49; purple, PPE-CO_2Na-108. Polymer concentration (polymer repeat units) = 5 μM, and the emission spectra were acquired with excitation at 380 nm.

In contrast to the red shift of the absorption maximum with increasing chain length, as shown in Figure 3b all of the CPEs exhibit essentially the same fluorescence emission spectrum, with a constant band maximum at 436 nm (0−0 band). This can be explained by the fact that, regardless of the CPE chain length, the singlet exciton undergoes efficient intrachain energy transfer to segments with a comparatively long conjugation length (lowest energy). Thus, although the absorption spectra indicate that the average conjugation length is shorter for the shorter chains, even relatively short CPE chains feature one or more segments that provide substantial conjugation for the fluorescent exciton. Another feature of interest is that the fluorescence quantum yield decreases significantly with increasing CPE chain length (see Table 2 and Figure 3b, where the fluorescence spectra are normalized according to the fluores-

Table 2. Photophysical Properties of CPEs in Methanol and Water Solution

	in methanol				in water			
	λ_{max}^{ab} (nm)	ϵ_{max} ($\times 10^4$) (M^{-1} cm^{-1})	λ_{max}^{em} (nm)	Φ_{FL}	λ_{max}^{ab}	ϵ_{max} ($\times 10^4$) (M^{-1} cm^{-1})	λ_{max}^{em} (nm)	Φ_{FL}
PPE-CO_2Na-7	404	3.6	436	0.64	408	3.3	520	0.14
PPE-CO_2Na-13	411	5.1		0.60	436	5.1		0.18
PPE-CO_2Na-35	417	5.8		0.32	438	6.5		0.09
PPE-CO_2Na-49	419	4.6		0.31	439	7.0		0.1
PPE-CO_2Na-108	432	5.1		0.15	440	6.8		0.04
PPE-CO_2Na-187	433	6.9		0.23	441	9.1		0.07

cence quantum yield). The fact that the fluorescence yield decreases with increasing CPE chain length may be the result of several factors. First, the possibility for the singlet exciton to undergo nonradiative decay via quenching by defects or other heterogeneity (e.g., conformation) increases with increasing CPE chain length. Second, the tendency for the CPE chains to aggregate increases with molecular weight, and it is well-known that the radiative decay rate of the "excimer-like" state in the aggregate is significantly less than for the molecularly dissolved chains.

The absorption and emission properties of the CPEs in water are dominated by the strong tendency of the chains to aggregate in aqueous solution (Figure S6). In particular, the absorption of PPE-CO_2Na-7 shows a major absorption band centered at 409 nm and a shoulder band at 437 nm. As the molecular weight of the CPEs increases, there is a negligible shift in the position of the 409 nm absorption, but there is a continuous increase in the relative intensity of the red-shifted band (ca. 440 nm) which is due to the CPE chain aggregates. The fluorescence spectrum of all of the CPEs appears as a broad, red-shifted and structureless band with $\lambda_{max} \approx 520$ nm coupled with a significantly lower quantum yield (0.04−0.18, Table 2) compared to that observed in MeOH.

Amplified Fluorescence Quenching. The fluorescence quenching of anionic CPEs by viologen derivatives with different charges or substituents was previously investigated by Heeger and Bazan,[7,8,44] and on the basis of this work, it is known that viologens quench via a photoinduced charge transfer mechanism.[45] Our previous work[14] on poly(phenylene ethynylene)-type CPEs demonstrated that quenching by the divalent cation dimethylviologen (MV^{2+}) is more efficient in water than in methanol because of enhanced interchain exciton migration in the CPE aggregates that are present in aqueous solution. We also reported that even in methanol solution chain aggregation is induced by the divalent cation MV^{2+}, and this effect plays an important role in enhancing the amplified quenching effect.[41] The MV^{2+}-induced aggregation is signaled by a bathochromic shift in the absorption spectra of the CPEs that occurs concomitant with addition of MV^{2+} to the polymer solution. Similar changes in the absorption spectra were observed when the quenching of the PPE-CO_2Na series by MV^{2+} was examined in MeOH solution (e.g., see Figure S7 for the spectra of PPE-CO_2Na-7 with addition of MV^{2+}), a finding which indicates that by analogy to our previous work the divalent quencher cation induces aggregation of the PPE-CO_2Na chains.

Since a primary objective of the present study is to explore the effect of CPE chain length on the amplified quenching efficiency, it is necessary to carry out quenching using monovalent cations in order to minimize the effects of quencher-induced aggregation. Thus, in the quenching studies outlined below, two monovalent, cationic viologen derivatives (MV^+ and HV^+, Chart 1) were used as quenchers. All of the quenching experiments were done in methanol, conditions in which the CPEs exist predominantly as "molecularly dissolved" chains. In addition, the CPE concentration was maintained at 5.0 μM (polymer repeat unit concentration) in order to minimize possible concentration-dependent aggregation. Quenching was evaluated using the Stern−Volmer (SV) equation with fluorescence intensity monitored at 436 nm. As shown in Figure 4a, the SV quenching plots for all the CPEs with MV^+ exhibit nearly linear correlations over the quencher concentration range from 0 to 3.2 μM. Stern−Volmer constants (K_{SV}) for the series of PPE-CO_2Na CPEs were extrapolated from linear fits of the SV plots, and the values are plotted as a function of chain length in Figure 4b. Stern−Volmer quenching was also carried out for HV^+,

Chart 1

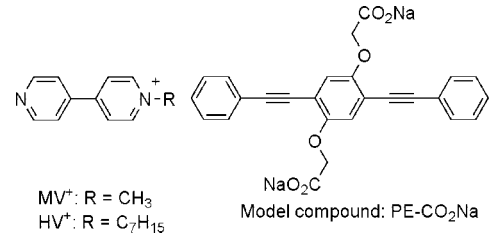

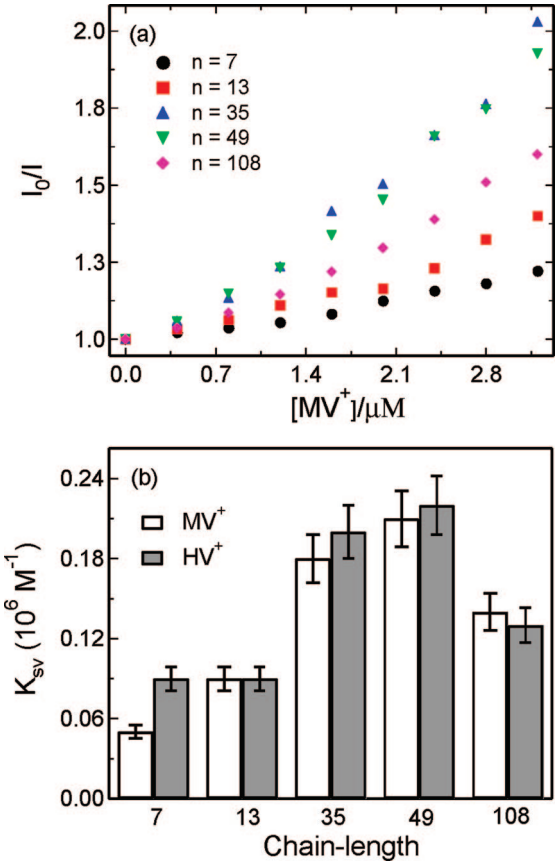

Figure 4. (a) Stern−Volmer plots of the series (polymer concentration = 5 μM) with MV^+: black, PPE-CO_2Na-7; red, PPE-CO_2Na-13; blue, PPE-CO_2Na-35; green, PPE-CO_2Na-49; purple, PPE-CO_2Na-108. (b) Comparison of the K_{SV} values obtained from SV plots for the series quenching by MV^+ and HV^+ in MeOH.

and the K_{SV} values for this quencher are also shown in Figure 4b. (In general, for the same polyelectrolyte, HV^+ shows a slightly higher quenching efficiency than MV^+ due to the solvophobic effect, as also observed by Heeger and co-workers.[8]) Inspection of the K_{SV} data plotted in the bar graph in Figure 4b shows that there is a large increase (~3-fold) of the quenching constant as the chain length increases from 7 to 35. However, increase of the chain length from 35 to 49 results in a negligible change in K_{SV}, indicating that the effect of chain length on the quenching efficiency saturates at ~40 polymer repeat units (corresponding to 80 phenylene ethynylene units).

Interestingly, a further increase of the chain length to 108 (PPE-CO_2Na-108) leads to a *decrease* in the observed K_{SV} value compared with that observed for the medium chain length CPEs (PPE-CO_2Na-35 and PPE-CO_2Na-49). As noted above, the tendency for CPEs to aggregate in methanol increases with chain length. In particular, for PPE-CO_2Na-108, it is apparent from the absorption and fluorescence spectra that a considerable fraction of the chains exist in an aggregated state (see Figure S8). Thus, when the MV^+ quencher is added to the CPE solution, there is a competition between quenching of the aggregates and the free polymer chains. Close inspection of the fluorescence spectrum of PPE-CO_2Na-108 as the solution is titrated with MV^+ (Figure S8) shows that the emission at 520 nm (aggregate emission) is quenched more efficiently compared with the emission at 436 nm (free polymer chains). Stern−Volmer analysis of the quenching at the two different fluorescence wavelengths affords two quenching constants: 7.9×10^5 M^{-1} (520 nm, aggregates) and 1.4×10^5 M^{-1} (436 nm, free polymer chains). The significantly larger quenching constant obtained for the aggregates reveals that the quenching is more efficient for the aggregates compared with the free polymer chains. Moreover, since there is a competition between quencher binding with free polymer and polymer aggregate, the observation of more efficient quenching for the aggregates suggests the origin of the apparent decrease in quenching efficiency for PPE-CO_2Na-108 relative to the shorter chain polymers reflected in the bar graph in Figure 4b. In particular, the MV^+ quencher may partition selectively into the aggregate "phase", reducing the amount of quencher available for quenching the free polymer chains.

The concept of the quenching amplification factor (AF) was originally proposed by Zhou and Swager[12] to provide a quantitative measure of the degree by which conjugation enhances the sensitivity of the quenching. The AF is defined as the ratio of K_{SV} for the polymer divided by K_{SV} for a structurally appropriate "model" monomer that features the same receptor and chromophore.[12,46] Assuming that the equilibrium constant for association of the quencher with the receptor (or ion-pair formation in the case of CPE−ionic quencher pairs) is the same for the polymer and the model monomer, the AF value provides a measure of the number of repeat units within a chain that are effectively quenched. Furthermore, since the efficiency of photoinduced charge transfer decreases strongly with distance, a quencher ion will only quench an exciton that is within one repeat unit of its binding site. Thus, the AF provides a measure of the number of polymer repeat units that are sampled (on average) by the singlet exciton during its lifetime.

In order to compute the AF values for the PPE-CO_2Na series, the Stern−Volmer constant for MV^+ quenching of the monomeric model compound PE-CO_2Na (Chart 1) was determined. As shown in Figure S9, in methanol solution the SV plot for MV^+ quenching of PE-CO_2Na is linear and affords a K_{SV} value of 4×10^3 M^{-1}. The AF values for the PPE-CO_2Na series were then obtained by dividing the K_{SV} value for each polyelectrolyte by K_{SV} for PE-CO_2Na, and the resulting values are presented as a bar graph in Figure 5. The amplified quenching of the

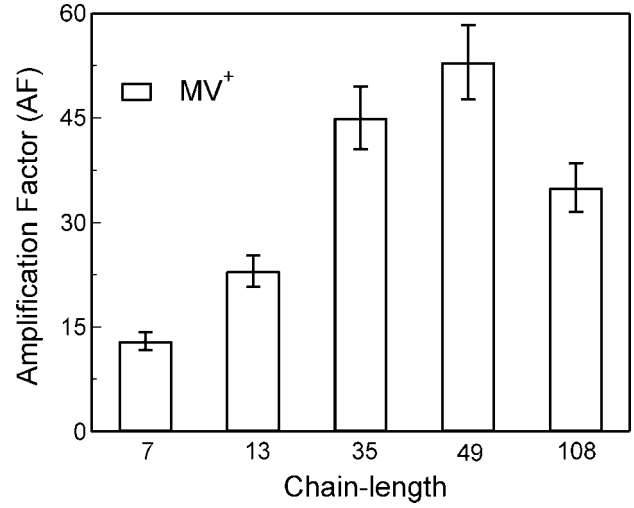

Figure 5. Amplification factors obtained by comparing the quenching of the series with the model compound by MV^+. See text for approach used to compute AF values.

polymer is evident compared with the model compound. Interestingly, the AF values steadily increase with chain length, saturating at ca. 53 for PPE-CO_2Na-49. (As discussed above, the apparent AF value decrease for PPE-CO_2Na-108 is due to polymer aggregation in solution.) Close inspection reveals that for the shorter CPEs the AF values exceed the DP (indeed they are almost twice of the chain length for PPE-CO_2Na-7 and PPE-CO_2Na-13). This is surprising because one would not expect the AF to exceed the polymer chain length, since the effective length of an individual "chromophore" cannot be less than a single polymer repeat unit. The larger than expected AF values may arise for several reasons. First, it is possible that the equilibrium constant for ion-pair formation is larger for the polymers compared with the model compound. Such an effect would also manifest as an effective increase in the AF. Second, we cannot rule out the possibility that there is some aggregation present even for the shortest chain CPEs.

Taken together the quenching data for the PPE-CO_2Na series suggests that for the shorter polymers the single MV^+ quencher effectively quenches an entire polymer chain up to a limit of ~40 polymer repeat units. A PPE-CO_2Na with 40 polymer repeat units contains ~80 phenylene ethynylene units, which corresponds to a length of ~40 nm (assuming the chain is in an extended conformation). Thus, the dependence of AF on the degree of polymerization for the PPE-CO_2Na series indicates that on average the singlet exciton is able to sample a polymer chain with a ~40 nm length within its lifetime (ca. 500 ps).[29] This result is qualitatively consistent with our earlier study of quenching of a sulfonate substituted poly(phenylene ethynylene) by cyanine dyes and with earlier work on organic soluble poly(phenylene ethynylene)s.[46]

Summary and Conclusion

In summary, we report the synthesis of a homologous series of CPEs with variable and controlled polymer chain length. The chain length is controlled by carrying out the step growth polymerization in the presence of a monofunctional (end cap) monomer. The homologous series of CPEs have a π-conjugated backbone structure based on poly(phenylene ethynylene) and feature carboxylate solubilizing side groups. The photophysical properties of the series of CPEs were investigated in methanol and water solutions and a clear picture emerges from the data; i.e., in methanol solution the shorter chain CPEs exist in a molecularly dissolved state, whereas for DP > 35 there is increasing evidence for the existence of aggregates. By contrast,

in aqueous solution regardless of chain length, all of the CPEs are aggregated.

By studying the quenching of the CPEs in methanol with monovalent quencher ions (MV^+ and HV^+), it is possible to discern the relationship between the amplified quenching effect and polymer chain length. The most significant result of the study is the observation that for low and moderate CPE chain lengths the amplification factor systematically increases, saturating at a value of ~50 for DP in the range of 35−50. This finding is consistent with earlier studies and suggests that in poly(phenylene ethynylene)s the singlet exciton is able to effectively sample a chain consisting of ≈80 phenylene ethynylene repeat units during its lifetime. In addition, the results of this study support the notion that the very high amplification factors (>1000) previously reported for CPE−ionic quencher systems arise mainly because of efficient interchain exciton diffusion within CPE aggregates.[5,14,47]

Acknowledgment. We acknowledge the United States Department of Energy, Office of Basic Energy Sciences (DE-FG-0296ER14617), for support of this work. We also thank Dr. Kye-Young Kim for assistance with graphics.

Supporting Information Available: Details of monomer synthesis; ^{1}H NMR of the precursor polymers and ^{1}H NMR and IR of the conjugated polyelectrolytes; absorption and fluorescence spectra of the series of CPEs in water; absorption spectra of PPE-CO_2Na-7 in methanol with MV^{2+}; absorption and emission spectra of PPE-CO_2Na-108 with the addition of MV^+; Stern−Volmer (SV) plot for the quenching of model compound (PE-CO_2Na) in MeOH by MV^+. This material is available free of charge via the Internet at http://pubs.acs.org.

References and Notes

(1) Shi, S. Q.; Wudl, F. *Macromolecules* **1990**, *23*, 2119–2124.
(2) Chen, L. H.; McBranch, D. W.; Wang, H. L.; Helgeson, R.; Wudl, F.; Whitten, D. G. *Proc. Natl. Acad. Sci. U.S.A.* **1999**, *96*, 12287–12292.
(3) Kim, I. B.; Dunkhorst, A.; Gilbert, J.; Bunz, U. H. F. *Macromolecules* **2005**, *38*, 4560–4562.
(4) Zhao, X. Y.; Liu, Y.; Schanze, K. S. *Chem. Commun.* **2007**, 2914–2916.
(5) Pinto, M. R.; Kristal, B. M.; Schanze, K. S. *Langmuir* **2003**, *19*, 6523–6533.
(6) Wang, J.; Wang, D. L.; Miller, E. K.; Moses, D.; Bazan, G. C.; Heeger, A. J. *Macromolecules* **2000**, *33*, 5153–5158.
(7) Wang, D. L.; Wang, J.; Moses, D.; Bazan, G. C.; Heeger, A. J. *Langmuir* **2001**, *17*, 1262–1266.
(8) Fan, C. H.; Hirasa, T.; Plaxco, K. W.; Heeger, A. J. *Langmuir* **2003**, *19*, 3554–3556.
(9) Liu, M.; Kaur, P.; Waldeck, D. H.; Xue, C. H.; Liu, H. Y. *Langmuir* **2005**, *21*, 1687–1690.
(10) Fan, C. H.; Plaxco, K. W.; Heeger, A. J. *J. Am. Chem. Soc.* **2002**, *124*, 5642–5643.
(11) Fan, C. H.; Wang, S.; Hong, J. W.; Bazan, G. C.; Plaxco, K. W.; Heeger, A. J. *Proc. Natl. Acad. Sci. U.S.A.* **2003**, *100*, 6297–6301.
(12) Zhou, Q.; Swager, T. M. *J. Am. Chem. Soc.* **1995**, *117*, 7017–7018.
(13) Lakowicz, J. R. *Principles of Fluorescence Spectroscopy*, 2nd ed.; Kluwer Academic/Plenum Publishers: New York, 1999.
(14) Tan, C. Y.; Pinto, M. R.; Schanze, K. S. *Chem. Commun.* **2002**, 446–447.
(15) Gaylord, B. S.; Wang, S. J.; Heeger, A. J.; Bazan, G. C. *J. Am. Chem. Soc.* **2001**, *123*, 6417–6418.
(16) Chen, L. H.; McBranch, D.; Wang, R.; Whitten, D. *Chem. Phys. Lett.* **2000**, *330*, 27–33.
(17) Tan, C. Y.; Alas, E.; Muller, J. G.; Pinto, M. R.; Kleiman, V. D.; Schanze, K. S. *J. Am. Chem. Soc.* **2004**, *126*, 13685–13694.
(18) Jiang, H.; Zhao, X. Y.; Schanze, K. S. *Langmuir* **2007**, *23*, 9481–9486.
(19) Fan, Q. L.; Zhou, Y.; Lu, X. M.; Hou, X. Y.; Huang, W. *Macromolecules* **2005**, *38*, 2927–2936.
(20) Chen, L. H.; Xu, S.; McBranch, D.; Whitten, D. *J. Am. Chem. Soc.* **2000**, *122*, 9302–9303.
(21) Dalvi-Malhotra, J.; Chen, L. H. *J. Phys. Chem. B* **2005**, *109*, 3873–3878.
(22) Abe, S.; Chen, L. H. *J. Polym. Sci., Part B: Polym. Phys.* **2003**, *41*, 1676–1679.
(23) Montano, G. A.; Dattelbaum, A. M.; Wang, H. L.; Shreve, A. P. *Chem. Commun.* **2004**, 2490–2491.
(24) Martin, R. E.; Diederich, F. *Angew. Chem., Int. Ed.* **1999**, *38*, 1350–1377.
(25) Zhou, Q.; Swager, T. M. *J. Am. Chem. Soc.* **1995**, *117*, 12593–12602.
(26) Cabarcos, E. L.; Carter, S. A. *Macromolecules* **2005**, *38*, 10537–10541.
(27) Dolbier, W. R.; Rong, X. X.; Xu, Y. L.; Beach, W. F. *J. Org. Chem.* **1997**, *62*, 7500–7502.
(28) Jones, G.; Jackson, W. R.; Choi, C.; Bergmark, W. R. *J. Phys. Chem.* **1985**, *89*, 294–300.
(29) Haskins-Glusac, K.; Pinto, M. R.; Tan, C. Y.; Schanze, K. S. *J. Am. Chem. Soc.* **2004**, *126*, 14964–14971.
(30) Barltrop, J. A.; Jackson, A. C. *J. Chem. Soc., Perkin Trans. 2* **1984**, 367–371.
(31) Asakura, N.; Hiraishi, T.; Kamachi, T.; Okura, I. *J. Mol. Catal. A: Chem.* **2001**, *174*, 1–5.
(32) Odian, G. *Principle of Polymerization*, 3rd ed.; John Wiley & Sons: New York, 1991.
(33) Kloppenburg, L.; Jones, D.; Bunz, U. H. F. *Macromolecules* **1999**, *32*, 4194–4203.
(34) Bunz, U. H. F. *Chem. Rev.* **2000**, *100*, 1605–1644.
(35) Sperling, L. H. *Introduction to Physical Polymer Science*; John Wiley & Sons: New York, 2001.
(36) Cotts, P. M.; Swager, T. M.; Zhou, Q. *Macromolecules* **1996**, *29*, 7323–7328.
(37) Schumm, J. S.; Pearson, D. L.; Tour, J. M. *Angew. Chem., Int. Ed.* **1994**, *33*, 1360–1363.
(38) Francke, V.; Mangel, T.; Mullen, K. *Macromolecules* **1998**, *31*, 2447–2453.
(39) Ricks, H. L.; Choudry, U. H.; Marshall, A. R.; Bunz, U. H. F. *Macromolecules* **2003**, *36*, 1424–1425.
(40) Huang, S. L.; Tour, J. M. *J. Am. Chem. Soc.* **1999**, *121*, 4908–4909.
(41) Jiang, H.; Zhao, X.; Schanze, K. S. *Langmuir* **2006**, *22*, 5541–5543.
(42) Tour, J. M. *Chem. Rev.* **1996**, *96*, 537–553.
(43) Kim, J.; Swager, T. M. *Nature (London)* **2001**, *411*, 1030–1034.
(44) Wang, D. L.; Wang, J.; Moses, D.; Bazan, G. C.; Heeger, A. J.; Park, J. H.; Park, Y. W. *Synth. Met.* **2001**, *119*, 587–588.
(45) Bock, C. R.; Meyer, T. J.; Whitten, D. G. *J. Am. Chem. Soc.* **1974**, *96*, 4710–4712.
(46) Thomas, S. W.; Joly, G. D.; Swager, T. M. *Chem. Rev.* **2007**, *107*, 1339–1386.
(47) Harrison, B. S.; Ramey, M. B.; Reynolds, J. R.; Schanze, K. S. *J. Am. Chem. Soc.* **2000**, *122*, 8561–8562.

MA800191Q